Physics of the Earth and Planetary Interiors 245 (2015) 15–25

Contents lists available at ScienceDirect

Physics of the Earth and Planetary Interiors

journal homepage: www.elsevier.com/locate/pepi

Variation of the Earth's magnetic field strength in South America during the last two millennia: New results from historical buildings of Buenos Aires and re-evaluation of regional data

Avto Goguitchaichvili [a,*], Juan Morales [a], Daniel Schavelzon [b], Carlos Vásquez [c], Claudia S.G. Gogorza [d], Daniel Loponte [e], Augusto Rapalini [f]

[a] Instituto de Geofísica, Universidad Nacional Autónoma de México, Unidad Michoacán, Campus Morelia, Laboratorio Interinstitucional de Magnetismo Natural, Mexico
[b] Centro de Arqueología Urbana, Universidad de Buenos Aires, Argentina
[c] Universidad de Buenos Aires – CBC, Buenos Aires, Argentina
[d] Centro de Investigaciones en Física e Ingeniería del Centro de la Provincia de Buenos Aires, (CIFICEN-CONICET), Tandil, Argentina
[e] Instituto Nacional de Antropología y Pensamiento Latinoamericano, CONICET, Argentina
[f] IGEBA – Universidad de Buenos Aires-IGEBA, Buenos Aires, Argentina

ARTICLE INFO

Article history:
Received 10 November 2014
Received in revised form 30 March 2015
Accepted 14 May 2015
Available online 19 May 2015

Keywords:
Earth's magnetic field
Secular variation
Archaeomagnetism
South America
Argentina
Buenos Aires

ABSTRACT

The causes of the systematic decay of the Earth's Magnetic Field strength since eighteen century have been a matter of debate during the last decade. It is also well known that such variations may have completely different expressions under an area characterized with strong magnetic anomalies, such as the South Atlantic Magnetic Anomaly. To fully understand these atypical phenomena, it is crucial to retrieve the past evolution of Earth's magnetic field beyond the observatory records. We report on detailed rock-magnetic and archeointensity investigations from some well-studied historical buildings of Buenos Aires city, located at the heart of the South Atlantic Magnetic Anomaly. Samples consist of bricks, tiles, fireplaces and pottery, which are considered as highly suitable materials for archaeointensity studies. The dating is ascertained by historical documents complemented by archeological constraints. Eighteen out of 26 analyzed samples yield reliable absolute intensity determinations. The site-mean archaeointensity values obtained in this study range from 28.5 to 43.5 μT, with corresponding virtual axial dipole moments (VADMs) ranging from 5.3 to 8.04 × 10^{22} Am^2. Most determinations obtained in the present study are in remarkable agreement with the values predicted by the time varying field model CALS10k.1b (Korte et al., 2011). For the older periods the recently available SHA.DIF.14 model (Pavon-Carrasco et al., 2014) seems to have greater resolution.

South American archaeointensity database now includes absolute intensities from 400 to 1930 AD based on 63 selected archaeointensity determinations. The data set reveals several distinct periods of quite large fluctuations of intensity. However, most data are concentrated into a relatively narrow interval from AD 1250 to AD 1450. At the beginning of the record, values between 400 AD and 830 AD match well with ARCH3k.1 model. Some general features may be detected: the time intervals from about AD 400 to 950 and 1150 to 1280 are characterized by a quite monotonic decrease of geomagnetic intensity, while some increase is observed from AD 950 to AD 1250. In contrast, a systematic intensity decay is detected from 1550 to 1930 in excellent agreement with the model prediction. No firm evidence of correlation between the climate changes over multi-decadal time scales and geomagnetic intensity was found for South America.

1. Introduction

The question about the possible influence of geomagnetic field variations on Earth's climate and biosphere has gained a great interest during the last decade. The Earth's magnetic field is currently fluctuating quite atypically. The dipole moment has decreased by about 10% since eighteen century. During a geomagnetic reversal or excursion the field strength tends to decrease to about 20% of its pre-transitional value. One may speculate that the observed decrease in the magnitude in the last centuries indicates a next reversal or excursion (Constable and Korte, 2006). It is

* Corresponding author.
E-mail address: avto@geofisica.unam.mx (A. Goguitchaichvili).

http://dx.doi.org/10.1016/j.pepi.2015.05.006
0031-9201/

however extremely hard to estimate the effect of such abnormal changes on our planet. On the other hand, the recent dipole decay may be partly due to changes in the field fluctuations beneath the South Atlantic Ocean, which is related to the growth of the South Atlantic Magnetic Anomaly (SAMA), an area in which the field at the Earth's surface is now about 35% weaker than would be expected (Jackson et al., 2000; Hartmann and Pacca, 2009).

To elucidate these fascinating phenomena and estimate the global evolution of the geomagnetic field, it is crucial to retrieve the past evolution of Earth́s magnetic field components. Geomagnetic observatories may be considered as reliable tools for recording the geomagnetic field. They perform continuous measurements of the magnitude and directions of the Earth's magnetic field over many years. Observatory data reveal how the field is changing on a wide range of timescales from seconds to centuries, and this is important for understanding processes both inside and outside the Earth. However, observatory records are very limited in South America offering only a discontinued data set for last 80 years or so. In this context, the remanent magnetization of the burned archeological artifacts should be regarded as valuable contribution to retrieve geomagnetic records beyond to instrumental measurements.

Archaeomagnetic data determined from burned materials are very unevenly distributed geographically. They are abundant for Europe (Genevey and Gallet, 2002; Schnepp and Lanos, 2005; Gómez-Paccard et al., 2006), but particularly poor in South America (Goguitchaichvili et al., 2011, 2012; Hartmann et al., 2011). Even so, these data represent about 2 per cent of the worldwide database (GEOMAGIA50.v3 (http://geomagia.gfz/potsdam.de, Donadini et al., 2006; Korhonen et al., 2008).). This scarcity is generally attributed to the lack of well constrained ages associated to archaeological artifacts. Most archaeomagnetic dating methods use two or three components of the remanent magnetization vector (inclination, declination, and occasionally intensity). It is therefore a pre-condition that samples are collected from *in situ* archaeological structures like kilns, hearths, baked floors and furnaces. Unfortunately, it is not always possible to assess whether an archeological feature is found undisturbed. The advantage of absolute geomagnetic intensity studies (palaeointensity or archaeointensity) is that no *in situ* material is required. The disadvantage is that while the determination of the paleofield direction from the stepwise demagnetization of a rock can usually be accomplished without complications, the determination of paleofield intensity is much more difficult (Coe et al., 1978).

In the present study we report new archaeointensity data from some well studied historical buildings of the city of Buenos Aires, located at the heart of SAMA. Samples consist of bricks, tiles, fireplaces and pottery which are considered as highly suitable material for absolute intensity determination.

2. Architectural context and sample description

The greatest problem in any archaeomagnetic study is the relationship between the samples and absolute ages which are usually estimated using alternative methods (archaeological context, thermoluminiscense, C^{14} etc.). In case of urban historical buildings it is quite unlike to have absolute radiocarbon dates and age estimation comes from historical documents, constructive (relative) stratigraphy and less likely archaeological context. It is now a general agreement among the archaeomagnetists worldwide that the source of historical documents (when available) is the most precise one and should be considered even more reliable than radiocarbon dating since the calibration needed for this last method sometime introduces very large error. All samples and their age estimations are provided by the 'Centro de Arqueologia Urbana' of the University of Buenos Aires (http://www.iaa.fadu.uba.ar/cau/, see also Schavelzon, 2000, 2001).

One of the most important cities in South America, Buenos Aires, with more than 10 million inhabitants has a long and interesting history. A first settlement at the present day site was established in 1536 by 'conquistador' Pedro de Mendoza because of its privileged location to control all trade in the region containing present-day Argentina, Paraguay, Uruguay and parts of Bolivia. Buenos Aires is also a city with the highest urban concentration in South America. The dynamics of accelerated growth produced enormous wealth destruction, particularly of the civil architecture. However, due to ideological factors and a rooted concept of progress, almost nothing from the 16th to the first half of the 19th century has survived (Schavelzon, 2000, 2001), which is already a true irreparable urban tragedy.

The samples analyzed in this study belong to three of the most famous historical buildings of Buenos Aires (Convento de Santa Catalina de Sena, Casa de la Calle San Juan 338 and Casa Ezcurra). The collection (Fig. 1) belongs to Center of Urban Archaeology under scientific supervision of Dr. Daniel Schavelzon who excavated all these samples analyzed in the present study.

2.1. Convento de Santa Catalina de Sena

Santa Catalina de Sena, located on the edge of the city, was an excellent example of convents and Churches of 18th century architecture. It is a pity that the building was not completely finished due to the financial problems. The eight meter rectangular pit structure (Fig. 1B) is a main characteristic feature of this site. It was filled not only with human detritus, but also with high liquid-absorption capacity construction material as well as with numerous ceramics pottery objects. Around the end of 18th century and very beginning of 19th, the building was reformed. Therefore, remains found in its interior should have a quite narrow chronology between AD 1750 and AD 1800.

It is interesting to note that the vast majority of the pottery found was locally produced and almost no presence of Spanish ceramic is detected. The samples (BA2-1A trough BA2-1F) analyzed here are most probably older than the convent itself and belong to the Guarani's indigenous tradition, decorated by brushing the outer side. Usually the regional archaeology has dated it as a post 17th century product, or a marker of that time. It seems that the same workers (the local Indians) who constructed the convent, manufactured these pottery objects themselves. A single radiocarbon dating (419 ± 84 B.P.) is available for this site.

2.2. Casa de la Calle San Juan 338

A quite similar chronology was established for the Casa de la Calle San Juan 338. Initially serving as a ranch, it is constructed of mud bricks (earth, adobe) with a fireplace on the floor dated at AD 1750. Thanks to the good stratigraphy of both floors and walls and to historical documents, a quite accurate reconstruction of all constructive stages is achieved until its demolition in 2005. The triangular fireplace found in the courtyard (Fig. 1C) was an exceptional case of preservation under three levels of bricks and tiles. It is worth mentioning that there is no evidence of indigenous population in Buenos Aires prior to the arrival of the Spaniards. Thus, there was no ceramic production at the site before 1580.

We analyzed three archaeological artifacts from this site: two bricks (BA2-3 and BA2-4) and a small piece (BA2-5) of a fireplace (Table 1). First two fragments are rather precisely dated while the sample from fireplace may have a questionable age (Table 1) estimation (see below for more detailed discussion). However, no archeomagnetic values were obtained from this sample due to

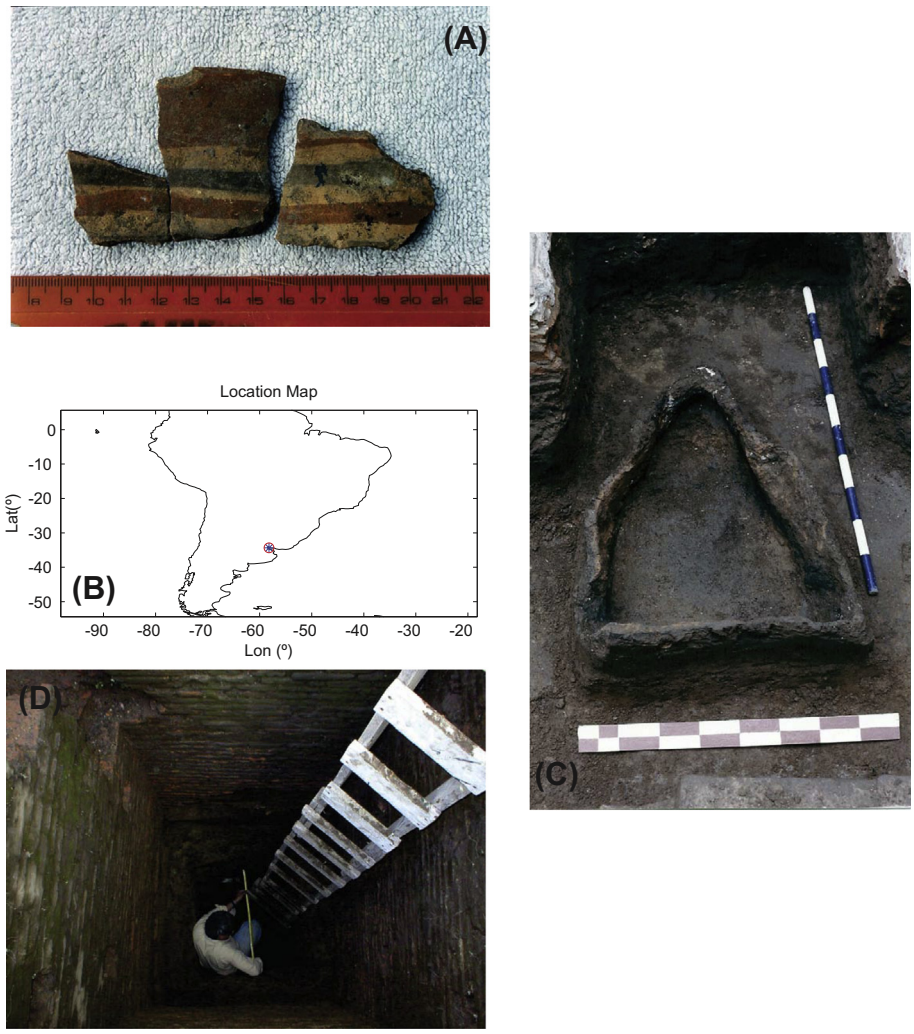

Fig. 1. Schematic location map and photographs of general archaeological features from some historical buildings of city of Buenos Aires. (A) Pottery of Indigenous origin at Casa Ezcurra, XVI century. (B) Location of Buenos Aires city in South America, (C) Fireplace 1790–1820 during the excavation of a house at San Juan 338, Buenos Aires, (D) Garbage pit of the Alfaro family in use 1830–1900 at San Isidro during excavations.

Table 1
Sample description and age estimations based on historical documents and urban archeological considerations. Also shown are age estimation inferred from archaeomagnetic dating (Pavón-Carrasco et al., 2011). In case of BA2-3 sample we use archaeomagnetic dating because the little age information available (see text for more details).

Lab. ID	Site	Sample type	Age estimation A.D.	Method	Inferred from archaeomagnetic dating CALS3 K.3
BA2-1	Santa Catalina	Pottery vessel	Around 1590	C^{14} and H. documents	1504–1596
BA2-2	Casa Ezcurra	Tile	1760–1820	Historical documents	1693–1833
BA2-3	San Juan 338	Brick (big)	1790–1820	Stratigraphy	1856–1900
BA2-4	San Juan 338	Brick (small)	1820–1830	Historical documents	1797–1895
BA2-5	San Juan 338	Fireplace	1790–1820	Stratigraphy	N.D.

the concave-up Arai-Nagata diagrams during the Thellier double-heating absolute intensity measurements (see below).

2.3. Casa Ezcurra

The so called 'Casa de Josefa Ezcurra' was a house originally constructed by the Jesuits apparently in AD 1750. After being expelled from the continent in AD 1776 its possession passed to Josefa Ezcurra, an important personality during the post revolutionary period. The excavation below allowed the finding of a late XVI century C14 dated stage and even contemporary materials, which offer a good correlation between constructive stages and burned material. This excavation also allowed also the identification of an enslaved African population revealed by its divinatory and religious objects, and also by its own ceramics. The tile sample measured in this study correspond to the initial stage of building and belongs to the time interval from around 1760 to 1820 (Schavelzon, 2000, 2001).

Samples analyzed in this study come from different parts of the mentioned houses and include bricks, tiles, pottery vessel and fireplace remains. Details of sample description with their chronological aspects are summarized in Table 1.

3. Magnetic properties and archaeointensity results

3.1. Rock-magnetism

Detailed rock-magnetic experiments are crucial to characterize the minerals carrying the remanence, to determine their thermal stability and to select the most suitable samples for absolute archaeointensity experiments. The set of rock-magnetic experiments consisted of (a) determination of hysteresis parameters, (b) isothermal remanent magnetization (IRM) acquisition curves and (c) continuous thermomagnetic curves (Fig. 2). All these measurements were carried out with an Advanced Variable Field Translation Balance (AVFTB) at the 'Laboratorio Interinstitucional de Magnetismo Natural (LIMNA)' of the National University of Mexico – Campus Morelia. Measurements were carried out on powdered specimens, and in each case, IRM acquisition and backfield curves were recorded first; then hysteresis curves were measured and finally samples were heated up in order to obtain M_S–T (saturation magnetization vs. temperature) curves.

Hysteresis parameters: M_S (saturation magnetization), M_{RS} (saturation remanence), B_C (coercivity) and B_{CR} (coercivity of remanence) were obtained from hysteresis and backfield curves. Analysis of the measurements was performed with the RockMagAnalyzer 1.0 software (Leonhardt, 2006). Four out of 5 samples studied yield consistent behaviour with no evidence of potbellied and/or wasp-waisted curves (Tauxe et al., 1996). A single, near magnetite ferrimagnetic phase seems to be the main magnetic carrier. Sample BA2-1 (pottery vessel) is a clear outlier (Fig. 2a) exhibiting an unusual hysteresis loop especially at high fields. Tentatively this may be interpreted as a wasp-waisted loop that may be obtained from a combination of single domain and superparamagnetic particles. The model reported in Fig. 5b of Tauxe et al. (1996) may probably produce such a kind of behaviour. Thus, our preferred interpretation is a combination of SD and SP grains. However, the most reliable interpretation is still open to debate.

Isothermal remanent magnetisation acquisition curves were recorded in a maximum applied field of approximately 0.8 T. More than 90% of saturation magnetization (SIRM) was reached with applied fields of less than 200 mT. The corresponding Ms–T curve indicates that Ti-poor titanomagnetite is the main carrier of magnetization. Curie temperatures determined using a technique developed by Moskowitz et al. (1981) varies from 515 °C to 540 °C.

3.2. Archaeointensity experiments

The five samples under study were further broken into at least 6 pieces and pressed into salt pellets to facilitate their treatment as standard paleomagnetic samples. The Thellier-Coe type experiments (Thellier and Thellier, 1959; Coe, 1967) were carried out using an ASC ScientificTD48-SC furnace; all heating/cooling runs were performed in air. Eleven temperature steps were distributed from 250 °C to 560 °C with reproducibility between two heating runs to the same nominal temperature better than 2 °C. The laboratory field strength was set to (30.0 ± 0.05) μT. Partial thermoremanent magnetization reinvestigations (pTRM checks) at each third temperature steps were added to the protocol.

The correction for the cooling rate effect needs to be applied on raw archaeointensity results. Morales et al. (2011) estimated that the original cooling time in an open kiln from 700 °C to 100 °C is about 2½ to 3 h., whereas average cooling time in laboratory (using a TD48 thermal demagnetizer with fan ON) ranges from 30 min to 45 min; this means a difference of near one order of magnitude between both cooling rates. According to experimental results on synthetic SD-type particles, this difference may produce an archaeointensity overestimation up to 7% (Fox and Aitken, 1980; McClelland-Brown, 1984). Still, systematic studies devoted to the cooling rate effect and the strength of magnetization for PSD grains (most abundant magnetic domain structure in rocks and burned archaeological artifacts) are limited. The cooling rate dependence of TRM was performed here following a modified procedure described in Chauvin et al. (2000); see also Morales et al. (2009), using a slow cooling time of 3 h. from 540 °C to 20 °C.

There is now a general agreement among the researchers and labs involved in absolute intensity that the great inconvenience of Thellier double-heating method is the numerous heatings (at least 22! in this study plus four pTRM checks plus three additional heatings for the cooling rate experiments) required, has potential to alter in some way the original remanent magnetization. The anisotropy correction requires at least 6 additional heatings at the high temperatures when usually less than 10% of original magnetization survives. Thus, there is almost ideal conditions for the eventual magneto-mineralogical alteration. In order to proceed to further archeomagnetic studies and to overcome this time-consuming procedure each of the ceramic, brick and tile fragments was arbitrary marked with parallel arrows on its internal or external flattening plane to create a reference orientation. Then each ceramic fragment was broken into "oriented" specimens of different sizes. Six specimens with the same type of shape and volume (1 cm^3) were chosen per ceramic, and were then embedded in

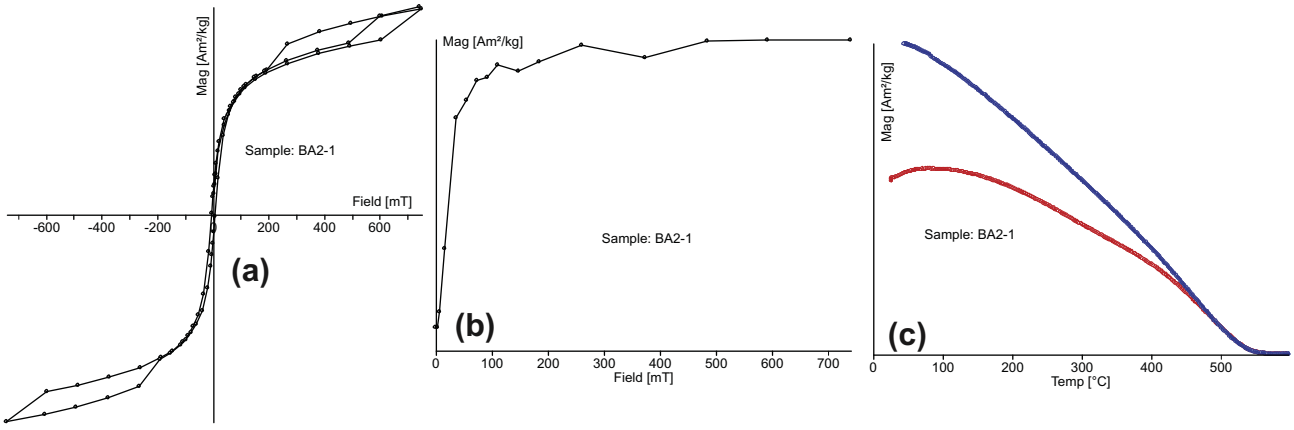

Fig. 2. Rock-magnetic properties of analyzed samples: (a) hysteresis plot, (b) isothermal remanent magnetization acquisition curve and (c) corresponding thermomagnetic (Ms–T) curve.

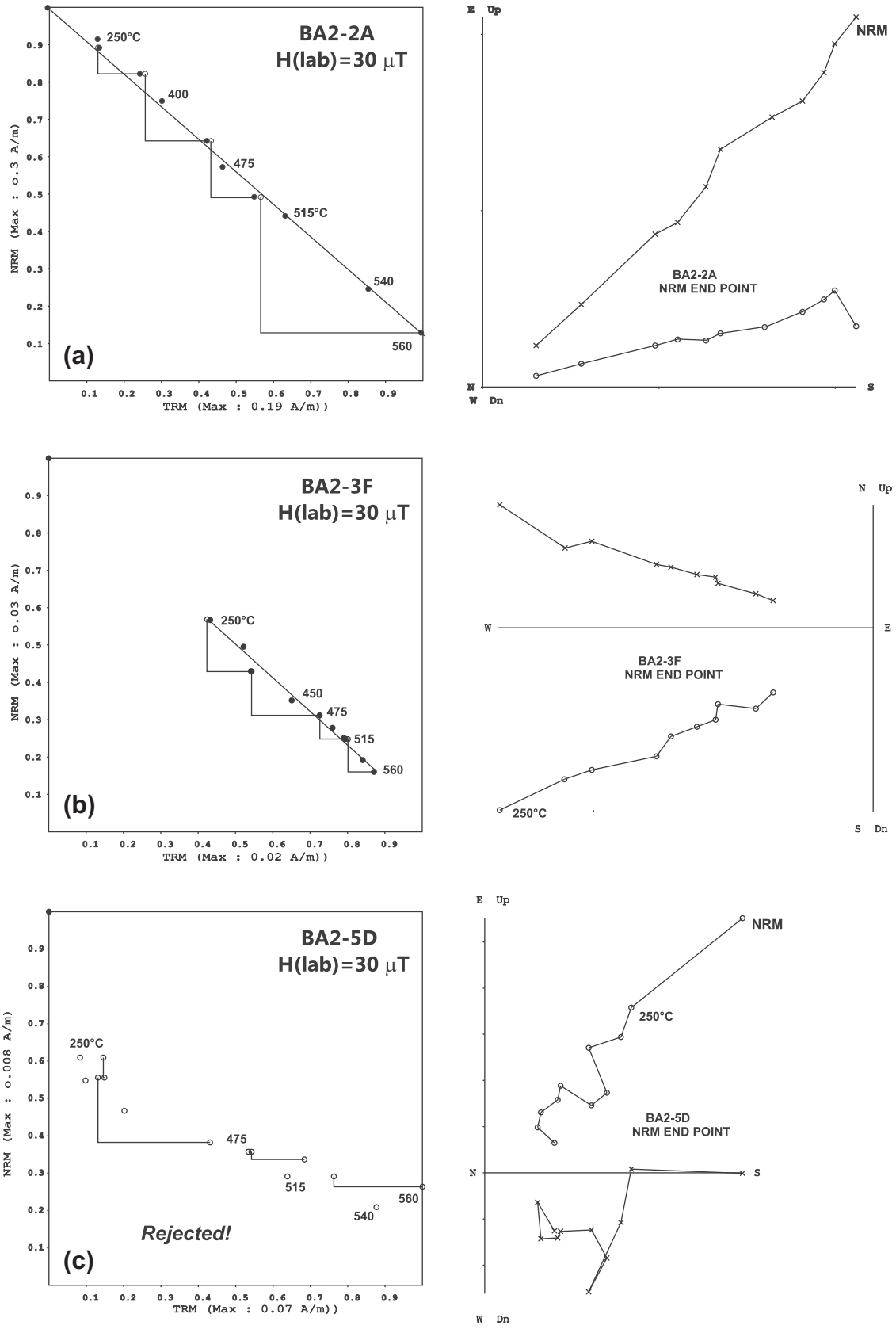

Fig. 3. Representative NRM–TRM plots (so-called Arai-Nagata plots) and associated orthogonal vector demagnetization diagrams for the representative samples. See text for more details.

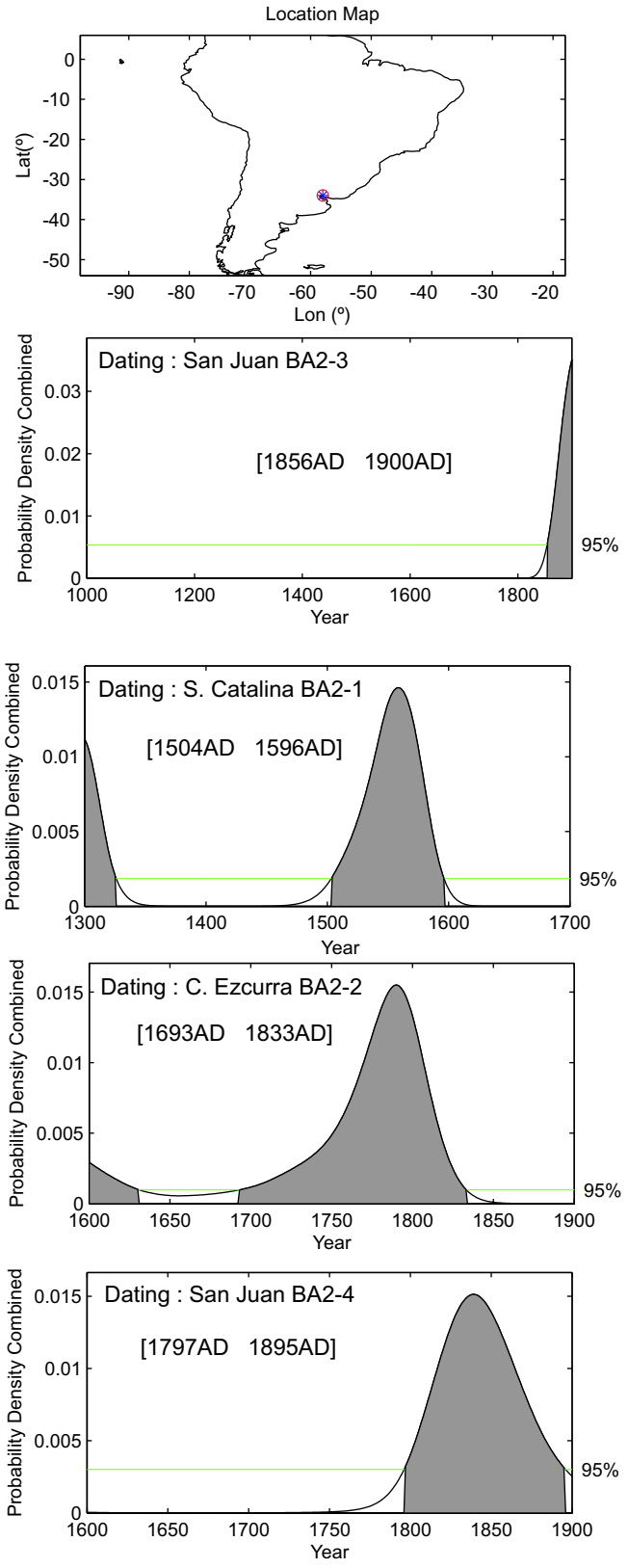

Fig. 4. Archaeomagnetic dating results for sample BA2-3 using a MATLAB tools provided by Pavón-Carrasco et al. (2011). See text for details.

ultra-pure salt (NaCl) pellets compressed with a non-magnetic hydraulic press in order to treat them as standard palaeomagnetic cores.

In addition we tried to perform standard TRM anisotropy measurements but on sister samples since almost all specimens inbedded in salt palets were broken and inusable due to several consecutive heatings. These measurements were carried out on only 20 samples because there was no unheated material available for the site San Juan 1 by inducing in the sample a pTRM (540 °C to room temperature) in six directions (i.e. $+x$, $+y$, $+z$, $-x$, $-y$, $-z$) in the presence of magnetic field of 30 μT (e.g. McCabe et al., 1985; Selkin et al., 2000; Chauvin et al., 2000). These measurements were performed on sister specimens used for archaeointensity determination. We calculated the anisotropy correction factor for each specimen according to Veitch et al. (1984). The anisotropy and CR corrected values are reported in Table 1, which attest that samples are magnetically nearly isotropic.

3.3. Archaeointensity results

The acceptance criteria for individual paleo or archeointensity determinations are now becoming standardized (Paterson, 2011, 2013, 2014) and may be summarized as follows: (1) Directions of natural remanent magnetization (NRM) end-points at each step obtained from Thellier double heating experiments have to fall along a reasonably straight line, trending toward to the origin in the interval chosen for archaeointensity determination. (2) No significant deviation of NRM directions towards the applied field direction should be observed. (3) At least five aligned TRM-NRM points on the Arai plot must be used (specimens suspected to carry considerable viscous remanent magnetization acquired *in situ* are rejected). (4) NRM fraction factor [*f*, Coe et al., 1978] $\geqslant$0.3. This means that at least 30 per cent of the initial NRM was used for archaeointensity determination. (5) A quality factor q (Coe et al., 1978) $\geqslant$4 (generally above 5), being $q = \frac{f*g}{\beta}\, g$, the gap factor (Coe et al., 1978) and β the relative standard error of the slope. (6) Archaeointensity results obtained from NRM-pTRM diagrams must not show an evident concave up shape, since in such cases remanence is probably associated with the presence of MD grains (Levi, 1977; Kosterov et al., 1998). (7) Positive pTRM checks, i.e., the deviation of 'pTRM' checks less than 15% comparing to original NRM-TRM step. In practice, the difference is less than 11%. It should be noted that at the first temperature steps when almost no NRM demagnetization happens some great pTRM check difference may be tolerated.

We underline here that the Coe (1967) modification of Thellier's (1959) original method used in present study should exclude the possibility to acquit a CRM (chemical remanent magnetization) or TCRM (thermochemical remanent magnetization) during the heatings in field. The crucial point is that CRM acquisition necessarily implies physico-chemical changes, which can result in an erroneous palaeointensity estimate. It is also important to note that even for samples which acquire a large CRM, the NRM/TRM diagram may be linear over an NRM fraction large enough to allow a palaeointensity determination (Coe et al., 1984). Thus, a specific CRM check is absolutely needed in complement to the usual checks of the Thelliers' method. As pointed out by Coe et al. (1984), a proper estimate of CRM intensity after heating at T requires consideration of not only the angular deviation a of the composite magnetization 'left' with respect to the direction of ChRM but also the angle between the ChRM direction and that of the applied field, which is assumed to correspond to the direction of CRM. In order to avoid any bias due to CRM, the ChRM direction in sample coordinates was obtained here from conventional AF treatment of another specimen from the same fragment. Let CRM(T) and NRM(T) be the CRM acquired and the NRM left (directed along the ChRM direction) after heating at T. The composite remanence measured at T is the vectorial sum of NRM(T) and CRM(T). We

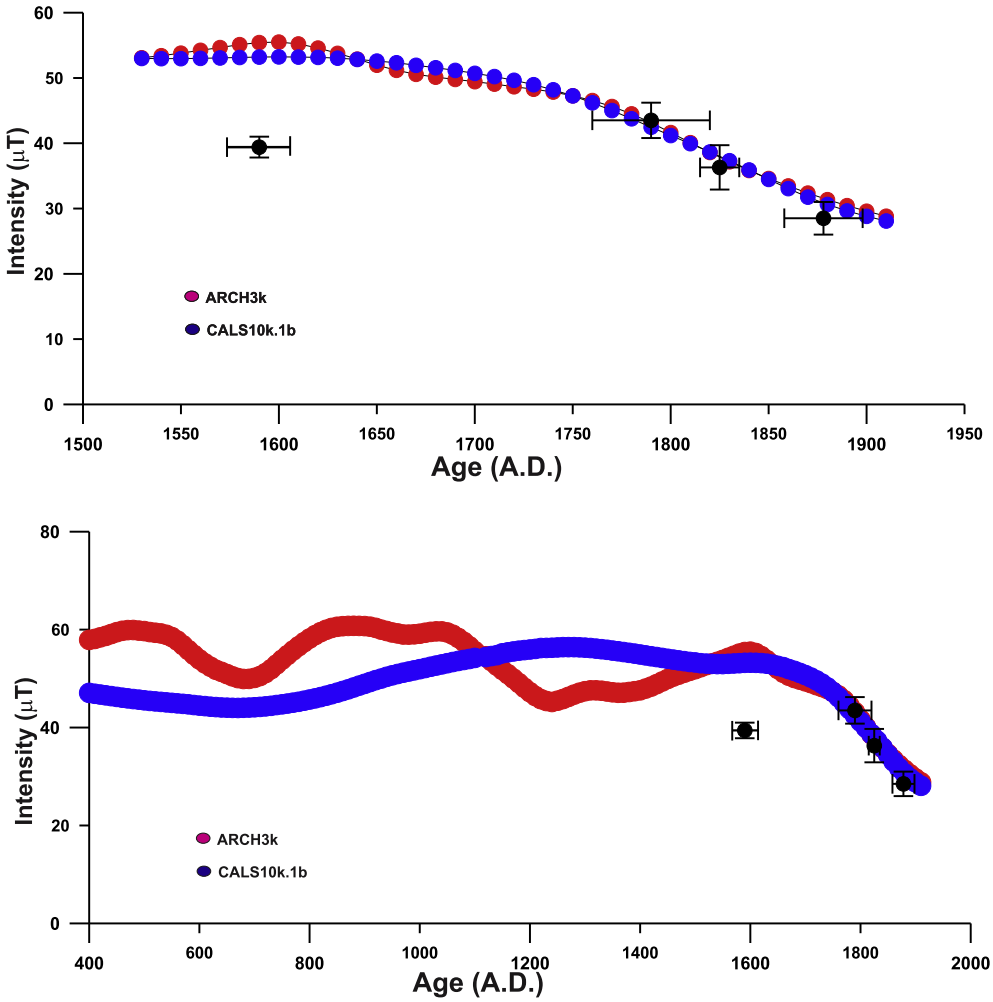

Fig. 5. Mean archaeointensity retrieved from this study against independently estimated ages together with ARCH3K and CALS10K.1b models (Donadini et al., 2009 and Korte et al., 2011). In case of BA2-3 sample we use archaeomagnetic dating because the little age information available (see text for more details).

define z as the ratio of CRM(T) to NRM(T) and although z varied from 0.12 to 0 great majority of values are under 0.1 even at high temperatures which attests that no important CRM acquisition is detected and thus no important deviation of NRM left points towards the applied field is detected. Even considering that NRM(T) are acquired in little bit higher field than in laboratory, these values remains relatively low. In the same context, we also calculate and report the angle γ between the direction of ChRM and that of the composite magnetization equal to NRM(T) if CRM(T) is zero obtained from the orthogonal plots derived from the Thellier paleointensity experiments (Table 1).

The best technical quality determinations were defined for Casa Ezcurra's samples (Fig. 3a) where all the criteria quoted above are fulfilled: the linearity of the Arai plots is observed along whole segments. Zijderveld diagrams are also linear, and NRM end directions point to the origin. pTRM checks are within the limits defined above. A small secondary viscous component can be present, but it is generally removed at low temperatures, around 250 °C. Samples of less quality, but nonetheless with acceptable determinations are illustrated in Fig. 3b. The Coe's quality factors are smaller and NRM-TRM points alignment are poorer. An example of a rejected sample is shown in Fig. 3c. Arai plots have a concave-up shape whereas Zijderveld projections show one linear component pointing to the origin.

In summary, eighteen out of 26 analyzed samples yield reliable absolute intensity determinations (Table 2). For these samples, the NRM fraction f used for determination ranges between 0.31 and 0.88 and the quality factor q from 2.7 to 32.3, being generally greater than 5. In few cases, we accepted lower q values because the corresponding intensity was very close to the site mean value. The great majority of f values are however higher than 0.4. The cooling rate correction generally reduced the standard deviation of the mean intensities. The fragment-mean archaeointensity values obtained in this study range from 28.5μT to 43.5 μT, with corresponding virtual axial dipole moments (VADMs) ranging from 5.3 to 8.04 $\times$ 10^{22} Am^2. For the data analysis obtained in this study, we prefer to describe the magnitude of the Earth's magnetic field in *microteslas* (local presentation), rather than in terms of the VADM (virtual axial dipole moment). The ideal case is naturally to present results in terms of the VDM (virtual dipole moment), but one should know the true magnetic inclination of samples, which is not the case here.

4. Discussion and concluding remarks

4.1. Archaeomagnetic dating applied to archaeointensity results

The age estimation of the samples BA2-1, BA2-2, and BA2-4 are based on radiocarbon dating and/or historical considerations whereas the age for both BA2-3 and BA2-5 samples were inferred by stratification (see Table 1). In order to provide more information

Table 2
Archaeointensity results at sample level. T_1–T_2: the temperature interval of intensity determination; N: the number of heating steps used for the intensity determination; g is the angle between the direction of ChRM and that of the composite magnetization equal to NRM(T) if CRM(T) is zero obtained from the orthogonal plots derived from the Thellier paleointensity experiments (please see text for more details), f, the fraction of NRM used for intensity determination; g: the gap factor; q: the quality factor as defined by Coe et al. (1978); H(corr): archeointensity value corrected for cooling rate effect.

Site	Sample	n	T_{min}–T_{max} (°C)	H corr (CR) (μT)	H corr (CR + AN) (μT)	σH	γ	f	g	q	VADM $10E^{22}Am^2$
S. Catalina	BA2-1A	8	300–540	40.8	39.4	4.8	5.3	0.73	0.81	6.7	7.6
	BA2-1B	8	250–515	36.3	34.8	2.2	4.8	0.58	0.77	7.4	6.7
	BA2-1C	9	250–540	40.4	40.1	3.2	5.0	0.72	0.82	6.1	7.5
	BA2-1D	8	250–515	39.7	40.6	3.3	6.2	0.59	0.82	6.4	7.4
	BA2-1E	7	300–515	39.6	38.2	2.6	3.4	0.48	0.77	6.6	7.3
	BA2-1F	8	250–515	39.8	37.8	3.3	4.9	0.65	0.83	4.5	7.4
			Mean =	39.4						Mean =	7.32
			s.d. =	1.6						s.d. =	0.31
C. Ezcurra	BA2-2A	11	20–560	41.8	43.5	1.4	2.2	0.85	0.86	32.3	7.7
	BA2-2B	10	250–560	45.9	44.9	1.2	1.6	0.88	0.84	28.4	8.5
	BA2-2C	11	20–560	45.4	44.6	1.8	2.9	0.88	0.86	18.8	8.4
	BA2-2D	8	300–540	47.3	46.3	3.4	3.3	0.65	0.82	10.7	8.8
	BA2-2E	9	250–540	42.1	40.8	1.3	1.5	0.68	0.85	20.8	7.8
	BA2-2F	9	250–540	40.6	41.3	1.7	2.2	0.72	0.83	16.7	7.5
	BA2-2G	11	20–560	41.2	N.A.	1.5	2.3	0.84	0.88	20.5	7.6
			Mean =	43.5						Mean =	8.04
			s.d. =	2.7						s.d. =	7.6
S. Juan 1	BA2-3A	*N/R*									
	BA2-3B	9	350–560	30.4	N.A.	4.6	6.6	0.41	0.68	2.7	5.6
	BA2-3C	8	300–560	25.8	N.A	1.8	6.2	0.34	0.75	3.2	4.8
	BA2-3D	9	250–560	26.9	N.A.	1.1	3.3	0.47	0.78	9.2	5.0
	BA2-3E	9	300–540	32.4	N.A.	3.4	7.6	0.31	0.77	4.2	6.1
	BA2-3F	10	250–560	27.2	N.A.	2.1	3.5	0.63	0.81	8.4	5.1
			Mean =	28.5						Mean =	5.3
			s.d. =	2.8						s.d. =	0.5
S. Juan 2	BA2-4A	9	250–540	36.4	38.2	3.5	6.3	0.46	0.82	4.9	6.7
	BA2-4B	9	300–560	29.1	31.6	3.8	4.6	0.48	0.84	6.2	5.4
	BA2-4C	8	250–515	37.6	37.7	4.1	9.8	0.42	0.83	2.7	7.0
	BA2-4D	7	250–500	38.4	37.5	2.9	6.2	0.36	0.77	4.7	7.1
	BA2-4E	10	20–560	35.1	36.4	1.8	4.3	0.79	0.81	11.2	6.5
	BA2-4F	8	20–515	38.2	36.8	3.8	8.4	0.56	0.74	4.6	7.1
	BA2-4G	8	250–540	39.1	37.9	1.6	5.2	0.35	0.77	7.5	7.2
			Mean =	36.3						Mean =	6.71
			s.d. =	3.4						s.d. =	0.6

about the age estimation, we can apply the archeomagnetic dating method to the different analyzed samples comparing the obtained archaeointensities with an intensity curve calculated, at the geographical position of the sampling site, from a paleomagnetic model. This was made by using the MATLAB tool of Pavón-Carrasco et al. (2011) and the global palaeomagnetic model CALS3k.3 of Korte et al. (2009). Please note that for the dating purposes we use CALS3k.3 model because it probably has higher resolution than CALS10k.1b (Korte et al., 2011). However, for the last 400 years both models yield similar values since they were constrained by the historical GUFM1 model of Jackson et al. (2000). Results are plotted in Fig. 4. For the sample BA2-1 (Santa Catalina site) the archaeomagnetic dating points out a much younger age than 1800 AD (associated chronology age for the Convento de Santa Catalina). However, this archaeomagnetic age (1504–1596 AD) agrees with the radiometric age of 419 ± 84 B.P. (calibrated age: 360 ± 70 B.P. using CALPAL or CALIB software) carried out in this sample. A good agreement is reached between the archaeomagnetic age and the established age for the site BA2-2 of "Casa Escurra". Finally, for the samples from "Casa de la Calle San Juan 338" we obtain different cases. A good correlation between the archaeomagnetic age and the historical constraint of the sample BA2-4. However, this is not the case of the sample BA2-3 where the original age estimation (based on stratigraphic and empirical features) was 1790–1820 AD and the archaeomagnetic dating provides a more recent age (from 1856 up to 1900). We prefer to use the archeomagnetic dating as the best estimation of the manufacturing time of this brick sample but taking into account that this sample does not have independent age estimation. Please, note also that the maximum of the time interval at 1900 is due the temporal limits used for dating. Since any archeomagnetic values were obtained from the last sample of "Casa de la Calle San Juan 338" (BA2-5) due to the concave up Arai-Nagata diagrams during the Thellier double-heating absolute intensity measurements, the archaeomagnetic dating was not possible.

4.2. New archaeointensity data from Argentina: comparison with the South America database and global models

The average results from the four samples are plotted on Figs. 5, 6 and 7, together with the predictions from the global models ARCH3k.1 (Korte et al., 2009), CALS10K.1b (Korte et al., 2011), and SHA.DIF.14k (Pavon-Carrasco et al., 2014) which cover the last 3 ka, 10 ka, and 14 ka respectively. These models are the latest developed using all the available palaeomagnetic data for their corresponding time intervals and applying the classical modeling approach, i.e. the spherical harmonic analysis in space and the penalized cubic B-splines in time. The ARCH3k.1 and SHA.DIF.14k models are only based on archaeomagnetic data (including lava flow data) and both model predictions agree for the last 3 ka, while the CALS10k.1b model includes lake sediment records. This last model is aimed to provide a robust representation of the large-scale field at the core-mantle boundary, but the ARCH3k.1 and SHA.DIF.14k models provides more variability in terms of both spatial and temporal resolutions (Korte et al., 2009; Pavón-Carrasco et al., 2014).

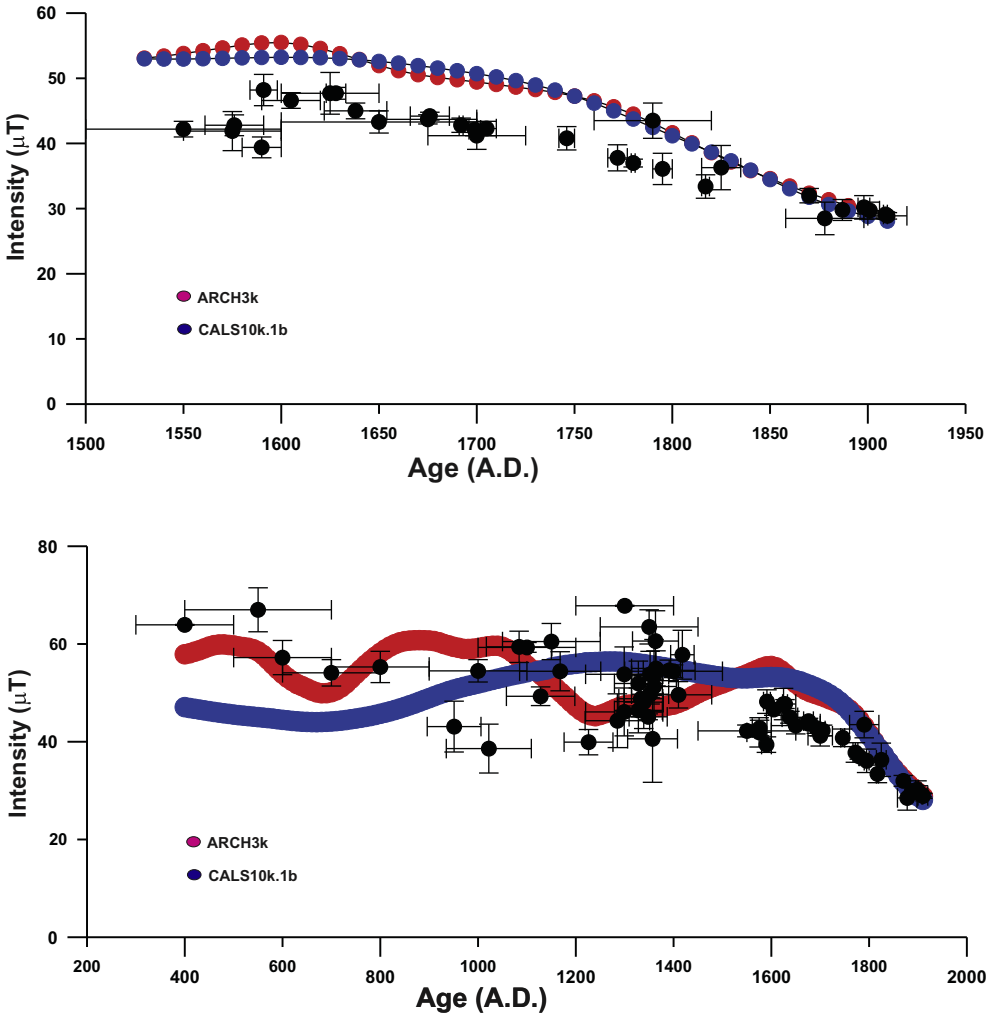

Fig. 6. Currently available, selected absolute intensity data from South America from 400 AD to 1930 AD. Also shown are the data derived from the CALS10K.b1 and ARCH3K model prediction at latitude and longitude of Buenos Aires.

A new geomagnetic field model for the Holocene – a so called SHA.DIF.14 (Pavon-Carrasco et al., 2014) seems to have greater resolution because it allows to analyze the behaviour of the geomagnetic field for the last 14,000 yr: from 12000 BC to 1900 AD. For the last 3 ka, the model predictions agree with those given by the global model ARCH3k.1 and the European model SCHA.DIF.3k. For older epochs, the new model presents a clear improvement in field resolution with respect to other current models of the geomagnetic field for the Holocene. The present study confirms and reinforces the superiority of this model against CALS10K.1b and ARCH3k.1 predictions. The absolute intensity value obtained here at about 1600 AD is a clear of outlier comparing to ARCH3k.1 and CALSK10K.1b while it agree reasonably well with the SHA.DIF.14K curve (Fig. 7a).

The regional data compilation includes results from Peru (Shaw et al., 1996), Argentina (Goguitchaichvili et al., 2011, 2012) and Brazil (Hartmann et al., 2010, 2011). There are some more data from South America but most of them do not meet any commonly acceptable criteria. For instance, no cooling rate and anisotropy corrections are performed and independent age determinations are very questionable. We did not selected data from northern Ecuador because it is very far away from the study area. We kept Peruvian data because they represent only available data for the region during the older time intervals. The Argentinean data were re-evaluated in terms of both intensity and age estimations and thus some unreliable determinations were discarded (Greco, 2012). One more record from Brazil (Hartmann et al., 2009) may be found in the Geomagia Database. Because no cooling rate and anisotropy corrections were applied to raw paleointensities, we decided to discard these results as well. All available South American data are shown on Fig. 6, together with the present study results. All Brazilian data are concentrated between AD 1580 and AD 1840 and show well defined monotonic decrease from about 45–35 μT. The same tendency is observed for ARCH3k.1, CALS10K.1b and SHA.DIF.14K (Figs. 6 and 7b) model predictions. However, Brazilian data are up to 20% lower than intensities inferred from the model. Let us note that all Peruvian and Brazilian date were relocated to Buenos Aires at 34°.36′ South and 58°24′ West. Thus, it is obvious that the systematic offset of the Brazilian and Peruvian results from the model cannot be due to the difference in dipole field strength at different latitudes. In contrast, Argentinean data between AD 1840 and AD 1930 agree almost perfectly to the models. This difference may be speculatively attributed to non-uniform distribution of South Atlantic Magnetic Anomaly. Considering the whole time-interval, the South American archaeointensity database now includes absolute intensities from AD 400 to AD 1930 based on 63 reliable (technically speaking) determinations. The data set shows several distinct periods of fluctuations of quite large intensity. However, most data are concentrated into a relatively narrow interval from AD 1250 to

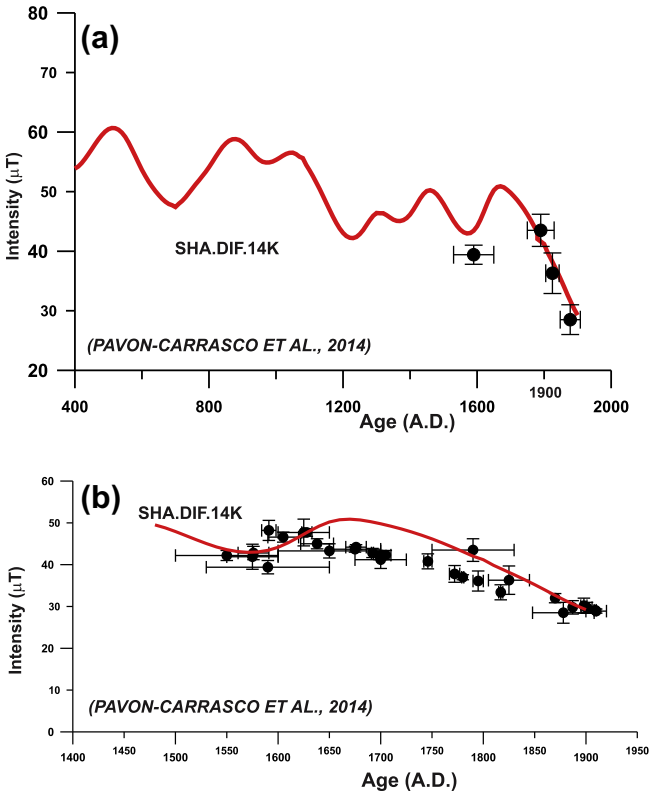

Fig. 7. (a) Mean archaeointensity obtained in this study compared to SHA.DIF.14K model prediction (Pavon-Carrasco et al., 2014) and (b) currently available selected absolute intensity data from South America between 1500 and 1900 AD compared to the intensity curve derived from the SHA.DIF.14K model prediction (Pavon-Carrasco et al., 2014).

AD 1450. At the beginning of the record, data between AD 400 and AD 830 match well with ARCH3k.1 model. Some general features may be detected: the time intervals from about AD 400 to AD 950 and AD 1150 to AD 1280 are characterized by a quite monotonic decrease of geomagnetic intensity, while some increase is observed from AD 950 to 1150. In contrast, a well-defined intensity decay is detected from AD 1550 to AD 1930 in excellent agreement with the model data. As suggested by Gallet et al. (2006) and Courtillot et al. (2007), these fluctuations may be correlated with climate changes over multi-decadal time scales. The cooling (warming) episodes are synchronous to the intensity increase (decrease) and seem to be influenced by the geomagnetic field through the modulation of the cosmic ray flux interacting with the atmosphere. However, in the case of South America, where no reliable climate record is available it is hard to make any firm conclusion. Stine (1994) reported a persistent warm climate from Patagonia between AD 1200 and AD 1350 and thus one should expect a considerable intensity decrease. The high dispersion of intensity data for this interval does not allow determining a firm tendency of absolute geomagnetic intensity. In addition, Argollo and Mourguiart (1995) report an evidence for a relatively large cooling interval from AD 1600 to AD 1900 in Bolivia (so-called a 'small ice age') based on paleoclimatic indicators of Titicaca Lake, in strong disagreement with South American archaeointensity data which show very consistent decay for the period involved.

Acknowledgments

Financial support was provided by 'Consejo Nacional de Ciencia y Tecnologia' - Mexico, projects129653 and UNAM PAPIIT IN105214.

References

Argollo, J. and P. Mourguiart (1995), Los climas cuaternarios de Bolivia, in Cambios Cuaternarios en América del Sur, edited by Argollo and Mourguiart, pp. 135–155.
Chauvin, A., Garcia, A., Lanos, Ph., Laubenheimer, F., 2000. Paleointensity of the geomagnetic field recovered on archaeomagnetic sites from France. Phys. Earth Planet. Inter. 120, 111–136.
Constable, C.G., Korte, M., 2006. Is Earth's magnetic field reversing? Earth Planet. Sci. Lett. 246, 1–16. http://dx.doi.org/10.1016/j.epsl.2006.03.038.
Coe, R.S., 1967. Paleointensities of the earth's magnetic field determined from Tertiary and Quaternary rocks. J. Geophys. Res. 72 (12), 3247–3262. http://dx.doi.org/10.1029/JZ072i012p03247.
Coe, R.S., Grommé, S., Mankinen, E.A., 1978. Geomagnetic paleointensities from radiocarbon-dated lava flows on Hawaii and the question of the Pacific non-dipole low. J. Geophys. Res. 83 (B4), 1740–1756. http://dx.doi.org/10.1029/JB083iB04p01740.
Courtillot, V., Gallet, Y., Le Mouël, J.L., Fluteau, F., Genevey, A., 2007. Are there connections between the Earth's magnetic field and climate? Earth Planet. Sci. Lett. 253, 328–339.
Donadini, F., Korhonen, K., Riisage, P., Pesonen, L.J., 2006. Database for Holocene geomagnetic intensity information, Eos. Trans. Amer. Geophys. Union 87, 137.
Donadini, F., Korte, M., Constable, C.G., 2009. Geomagnetic field for 0–3 ka: 1. New data sets for global modeling. Geochem. Geophys. Geosyst. 10, Q06007. http://dx.doi.org/10.1029/2008GC002295.
Fox, J.M.W., Aitken, M.J., 1980. Cooling rate dependence of the thermoremanent magnetization. Nature 283, 462–463.
Gallet, Y., Genevey, A., Le Goff, M., Fluteau, F., Eshraghi, S.A., 2006. Possible impact of the Earth's magnetic field on the history of ancient civilizations, Earth Planet. Sci. Lett. 246, 17–26.
Genevey, A., Gallet, Y., 2002. Intensity of the geomagnetic field in Western Europe over the past 2000 years: new data from ancient French pottery. J. Geophys. Res. 107 (B11), 2285. http://dx.doi.org/10.1029/2001JB000701.
Goguitchaichvili, A., Greco, C., Morales, J., 2011. Geomagnetic field intensity behavior in South America between 400 AD and 1800 AD: first archeointensity results from Argentina. Phys. Earth Planet. Inter. 186, 191–197.
Goguitchaichvili, A., Loponte, D., Morales, J., Acosta, A., 2012. The archaeointensity of the rarth's magnetic field retrieved from pampean ceramics (South America). Archaeometry 54 (2), 388–400.
Gómez-Paccard, M., Chauvin, A., Lanos, Ph., Thiriot, J., Jimenez-Castillo, P., 2006. Archeomagnetic study of seven contemporaneous kilns from Murcia (Spain). Phys. Earth Planet. Inter. 157, 16–32.
Greco, C., 2012. Integración de datos arqueológicos, radiocarbónicos y geofísicos para la construcción de una cronología de Yocavil y alrededores, (Ph.D. thesis), University of Buenos Aires, 288 pp.
Hartmann, G., Genevey, A., Gallet, Y., Trindade, R., Etchevarne, C., Le Goff, M., Afonso, M.C., 2010. Archeointensity in Northeast Brazil over the past five centuries, Earth Planet. Sci. Lett. 296, 340–352.
Hartmann, G., Genevey, A., Gallet, Y., Trindade, R., Le Goff, M., 2011. New historical archeointensity data from Brazil: evidence for a large regional non-dipole field contribution over the past few centuries, Earth Planet. Sci. Lett. 306, 66–77.
Hartmann, G.A., Pacca, I.G., 2009. Time evolution of the South Atlantic Magnetic Anomaly. Annals Brazil. Acad. Sci. 81, 243–255.
Hartmann, G.A., Trindade, R.I.F., Goguitchaichvili, A., Etchevarne, C., Morales, J., Afonso, M.C, 2009. First archeointensity results from Portuguese potteries (1550–1750 AD). Earth Planets Space 61, 93–100.
Jackson, A., Jonkers, A.R.T., Walker, M.R., 2000. Four centuries of geomagnetic secular variation from historical records. Phil. Trans. R. Soc. Lond. A 358, 957–990.
Korhonen, K., Donadini, F., Riisager, P., Pesonen, L.J., 2008. GEOMAGIA50: an archeointensity database with PHP and MySQL. Geochem. Geophys. Geosyst. 9.
Korte, M., Donadini, F., Constable, C.G., 2009. Geomagnetic field for 0-3 ka: 2. A new series of time-varying global models. Geochem. Geophys. Geosyst. 10, Q06008. http://dx.doi.org/10.1029/2008GC002297.
Korte, M., Constable, C.G., Donadini, F., Holme, R., 2011. Reconstructing the Holocene geomagnetic field, Earth Planet. Sci. Lett. 312, 497–505.
Kosterov, A.A., Perrin, M., Glen, J.M., Coe, R.S., 1998. Paleointensity of the Earth's magnetic field in Early Cretaceous time: the Parana Basalt, Brazil. J. Geophys. Res. 103 (B5), 9739–9753. http://dx.doi.org/10.1029/98JB00022.
Leonhardt, R., 2006. Analyzing rock magnetic measurements: the RockMagAnalyser1.0 software. Comput. Geosci. 32 (9), 1420–1431.
Levi, S., 1977. The effect of magnetite particle size on paleointensity determinations of the geomagnetic field. Phys. Earth Planet. Inter. 13, 245–259.
McCabe, C., Jackson, M., Ellwood, B., 1985. Magnetic anisotropy in the Trenton limestone: results of a new technique, anisotropy of anhysteric susceptibility. Geophys. Res. Lett. 12, 333–336.
McClelland-Brown, E., 1984. Experiments on TRM intensity dependence on cooling rate. Geophys. Res. Lett. 11 (3), 205–208.
Morales, J., Goguitchaichvili, A., Acosta, G., Gonzalez, T., Alva-Valdivia, L., Robles-Camacho, J., Hernadez-Bernal, Ma., 2009. Magnetic properties and archeointensity determination on some Pre-Columbian potteries from Chiapas, Mesoamerica. Earth Planets Space 61, 83–91.
Paterson, G.A., 2013. The effects of anisotropic and non-linear thermoremanent magnetizations on Thellier-type paleointensity data. Geophys. J. Int. 193, 694–710. http://dx.doi.org/10.1093/gji/ggt033.

Paterson, G.A., 2011. A simple test for the presence of multidomain behaviour during paleointensity experiments. J. Geophys. Res. 116, B10104. http://dx.doi.org/10.1029/2011JB008369.

Paterson, G., Tauxe, L., Biggin, A., 2014. On improving the selection of Thellier-type paleointensity data. Geochem. Geophys. Geosyst. 15 (89), 1059–1069. http://dx.doi.org/10.1029/JB089iB02p01059.

Pavon-Carrasco, F.J., Osete, M.L., Torta, J.M., De Santis, A., 2014. A geomagnetic field model for the Holocene base don archaeomagnetic and lava flow data, Earth Planet. Sci. Lett. 388, 98–109.

Morales, J., Goguitchaichvili, A., Aguilar-Reyes, B., Pineda-Duran, M., Camps, P., Carvallo, C., Calvo-Rathert, M., 2011. Are ceramics and bricks reliable absolute geomagnetic intensity carriers?. Phys. Earth Planet. Inter. 187, 310–321. http://dx.doi.org/10.1016/j.pepi.2011.06.007.

Moskowitz, B.M., 1981. Methods for estimating Curie temperatures of titanomagnetites from experimental Js-T data, Earth Planet. Sci. Lett. 53, 84–88.

Pavón-Carrasco, F.J., Rodríguez-González, J., Osete, M.L., Torta, J.M., 2011. A Matlab tool for archaeomagnetic dating. J. Archaeol. Sci. 38, 408–419.

Schavelzon, D., 2000. The historical archaeology of Buenos Aires: a city at the end of the world. Kluwer Academic, Plenum Press, New York.

Schavelzon, D. (2001), Catálogo de cerámicas históricas de Buenos Aires (siglos XVI-XX) con notas sobre la región del Río de la Plata, CD, Fundación para la Investigación del Arte Argentina y Telefónica- FADU, Buenos Aires.

Schnepp, E., Lanos, P., 2005. Archaeomagnetic secular variation in Germany during the past 2500 years. Geophys. J. Int. 163, 479–490. http://dx.doi.org/10.1111/j.1365-246X.2005.02734.x.

Selkin, P.A., Gee, J.S., Tauxe, L., Meurer, W.P., Newell, A.J., 2000. The effect of remanence anisotropy on paleointensity estimates: A case study from the Archean stillwater complex, Earth Planet. Sci. Lett. 183, 403–416.

Shaw, J., Walton, D., Yang, S., Rolph, T.C., Share, J.A., 1996. Microwave archaeintensities from Peruvian ceramics. Geophys. J. Int. 124, 241–244.

Stine, S., 1994. Extreme and persistent drought in California and Patagonia during medieval time. Nature 369, 546–549.

Tauxe, L., Mullender, T.A.T., Pick, T., 1996. Pot–bellies, wasp–waists and superparamagnetism in magnetic hysteresis. J. Geohys. Res. 101, 571–584.

Thellier, E., Thellier, O., 1959. Sur l'intensité du champ magnétique terrestre dans le passé historique et géologique. Ann. Geophys. 15, 285–376.

Veitch, J., Hedley, I., Wagner, J.J., 1984. An investigation of the intensity of the geomagnetic field during roman times using magnetically anisotropic bricks and tiles. Arch. Sci., Geneve 37, 359–373.